SCIENTIFIC HORIZONS

Journal homepage: https://sciencehorizon.com.ua

Scientific Horizons, 25(1), 9-20

UDC 62-932.4
DOI: 10.48077/scihor.25(1).2022.9-20

Modelling of Piling Technology by Vibroimpact Device with Hydropulse Drive

Yaroslav Ivanchuk*, Oleksandr Manzhilevskyy, Ruslan Belzetskyi, Oleksandr Zamkovyi, Roman Pavlovych

Vinnytsia National Technical University
21021, 95 Khmelnytske Shose Str., Vinnytsia, Ukraine

Article's History:
Received: 16.02.2022
Revised: 14.03.2022
Accepted: 15.04.2022

Suggested Citation:
Ivanchuk, Ya., Manzhilevskyy, O., Belzetskyi, R., Zamkovyi, O., & Pavlovych, R. (2022). Modelling of piling technology by vibroimpact device with hydropulse drive. *Scientific Horizons*, 25(1), 9-20.

Abstract. Based on the analysis of the developed mathematical model, this paper proposes optimal operating modes of the vibroimpact device to ensure the intensification of driving construction piles. It is an original design of a modern, highly efficient device for driving construction piles, equipped with a compact, powerful hydraulic impulse drive unit. To develop a mathematical model of the construction pile driving technology, the following methods were used: mechanoreological phenomenology, hydrodynamics, and generalised laws of mechanics. Mathematical models of the dynamics of technological processes of driving construction piles with a vibroimpact device are improved based on a hydraulic impulse drive unit in the form of a spatial non-stationary formulation of the problem and integral equations of dynamic characteristics of the moving elements of the drive unit. The study obtained the distribution of the pressure and velocity of the working fluid in the hydraulic unit of the vibroimpact device, as well as changes in the kinematic parameters of the elements of the technological equipment based on the mathematical model developed by the finite volume method, using numerical modelling and high-performance computer systems. Optimal modes of operation of a hydraulic impulse drive of a vibroimpact device are proposed to provide an intensification of the construction pile driving technology. It was found that when low-frequency vibration is applied, the driving of construction piles is intensified. Application of a hydraulic impulse drive that is based on two-stage vibration excitation allowed implementing the vibroimpact modes of the device. The average pile driving speed with a vibroimpact interaction is five times higher compared to conventional driving methods

Keywords: impulse, impact, vibration, mathematical model, hydraulic drive, valve, construction pile

*Corresponding author

INTRODUCTION

The growth of construction volumes is an essential sign of development as a separate construction industry, and of the country in general. Due to the large volume of housing and industrial construction, arises a need to build more structures in unfavourable soil conditions, which requires the use of special means, that often complicate and increase the cost of the construction process of facilities and buildings. The tendency to reduce these costs and the continuous advance of construction technology are leading to a wider introduction of pile foundations. That is why the problem of satisfying the increased requirements for reducing the cost of construction and increasing labour productivity by increasing the efficiency of the construction pile driving is relevant and acute (Bullock & William, 2001).

The main and the best way to intensify the pile driving is the use of vibroimpact loads (Glushak *et al.*, 1992). Vibroimpact (VI) load is created by a hammer equipped with a hydraulic impulse drive (HID) (Iskovych-Lototsky *et al.*, 2018a), the advantages of which include the intensification of the flow of several technological processes, ensuring optimal load parameters and high-quality results of technological processing (Fossen & Nijmeijer, 2012). However, the practices of using impact machines necessitated the solution of some issues, understanding which is impossible without analysing the effect of impact pulses on the object, as well as without analysing the dynamics of attachment equipment and the entire machine under the effect of loads from the working impact mechanism (Ivanchuk, 2020). Currently, mathematical modelling of physical processes is common (Guang & Min, 2005), using which allows deeply and fully exploring the influence of design and mode factors on the main characteristics of the construction equipment operation, to outline particular ways of their improvement while considerably reducing the amount of experimental research (Kang *et al.*, 2008). Despite the complexity of the calculations and the assumptions made in the mathematical description of the workflow, which can be clarified upon the accumulation of experimental data, the perspective of using such models for the development of effective structures of the VI attachments equipment for construction based on HID for pile driving, is evident (Ivanchuk, 2020).

The purpose of this article is to increase the efficiency of the theoretical study of the pile driving technology through the development of promising mathematical models of the physical processes of operating the hinged construction HID-based VI equipment. This will allow achieving several high-quality practical results: increasing the reliability of determining the operating characteristics upon designing a hydraulic drive; the possibility of developing systems with improved operational characteristics; reducing the time spent on development of certain technologies.

To achieve this purpose, the following *tasks* were solved:

– to improve the mathematical model of the pile driving technology based on a pre-made design of the developed hinged HID-based VI device;

– to determine the hydrodynamic parameters of the working fluid in the HID, which will allow analysing the operating modes of the hinged pile driving VI equipment;

– to determine the operating parameters of the HID to identify the efficient operating modes of the pile driving technology with a hinged VI device.

THEORETICAL OVERVIEW

The main apparatus of the mathematical modelling of VI processes includes exact methods of nonlinear mechanics based on adjustment solutions (Alessandro, 2016), describing adjacent intervals of movements of the executive body. These methods allowed thoroughly investigating the complex dynamic picture of the movements of several VI machines and revealing many of their inherent fundamental properties. However, the use of these methods for creation of mathematical models of a wide range of HID-based VI systems is laborious and limited by the scope of their application, especially when the dimension of the systems is increased, as well as when it is necessary to consider added nonlinear factors and the complication of the nature of disturbances from the action of non-periodic and random forces. A generally accepted approach for modelling VI systems is the asymptotic representation of solutions according to the degrees of a small parameter (Voskresenskiy, 2001) upon analysing the fundamental harmonic components of fluctuation. It is based on the selection of simpler ratios from their general mathematical description, while transitioning to spectral representations (Li *et al.*, 2019) and ideas of equivalent linearisation (Jörg *et al.*, 2010) but does not allow finding an acceptable mathematical model for vibration systems. This necessitates the development of new methods and approaches to create standard mathematical models of VI systems for a wide range of VI equipment.

The increase in speed, energy saturation, and compactness of the HID for VI machines are greatly influenced by the physical parameters of the energy carrier (working fluid) and the design parameters of the pressure pulse generator (PPG) (Iskovych-Lototsky *et al.*, 2018a), which provides control of the function of VI equipment. This leads to the development of mathematical models in the form of systems of differential equations of motion of the structural HID elements (Shatokhin *et al.*, 2019) based on an artificial dynamic model with the given coefficients for the oscillatory system. The practical implementation of the given approach is possible only for mathematical models mainly of low-dimensionality and describes the properties of objects in a narrow range of variation of operating

parameters such as the amplitude and oscillation frequency of the impulse drive elements. Available practices indicate that to overcome these difficulties, it is necessary to formulate a new objective of mathematical modelling of the pile driving technology by VI machines in a spatial non-stationary form. There is a need to develop new, more comprehensive and adequate mathematical models based on a system of differential equations in partial derivatives with coefficients in the form of integral functions of independent variables (Iskovych-Lototsky *et al*., 2018b). At present, he possibility of replacing a physical experiment with a numerical one, involving the use of computer modelling methods, is still a relevant issue.

MATERIALS AND METHODS

This paper presents an original methodology of mathematical and computer modelling of the pile driving technology by HID-based VI systems, considering the specific features of this class of objects, to ensure high design efficiency of a corresponding type of technical systems:

1. Based on the design methodology of road-building machinery with HID, an effective design of a hinged VI device has been developed, wherein a two-stage pulsator valve is used as a vibration exciter (Iskovych-Lototsky *et al*., 2018a; Iskovych-Lototsky *et al*., 2018b).

2. Based on a systems-technical approach (Barkan, 1952; Manzhilevsky, 2019; Iskovych-Lototsky *et al*., 2018b), structural and functional connections between the components of the hinged VI device were synthesised, which allowed determining the interconnection between the state parameters of the HID subsystems with the quality readings of the technological object.

3. Dynamic characteristics of the movable functional objects of the HID are described using linear inhomogeneous second-order differential equations, where the free term function is presented in the form of linearised functions of external forces, and the linearised coefficients express both elastic and dissipative force connections of the drive elements and rheological properties of the processing environment.

4. Mathematical model of the movement of functional objects of the HID is supplemented with a mathematical model of the working fluid movement, based on the system of nonlinear differential equations, in partial of the derivatives of Navier-Stokes and the continuity conditions for viscous fluids.

5. The developed mathematical model of the pile driving technology is implemented using separate software packages, which implement a corresponding numerical calculation method for solving mathematical models involving simulation modelling methods.

6. The analysis of the results of computer modelling of the dynamic processes of the HID-based VI system was carried out, which allowed determining the dynamic characteristics of the PPG function to determine the implementation of effective VI modes of operation.

RESULTS

For the pile driving technology (Barkan, 1952), a hinged HID-based VI device was developed, where a two-stage pulsator valve is used as a vibration exciter (Iskovych-Lototsky *et al*., 2018a; Iskovych-Lototsky *et al*., 2018b). The CAD software was used to develop a three-dimensional model of a mounted HID-based VI attachment (Fig. 1).

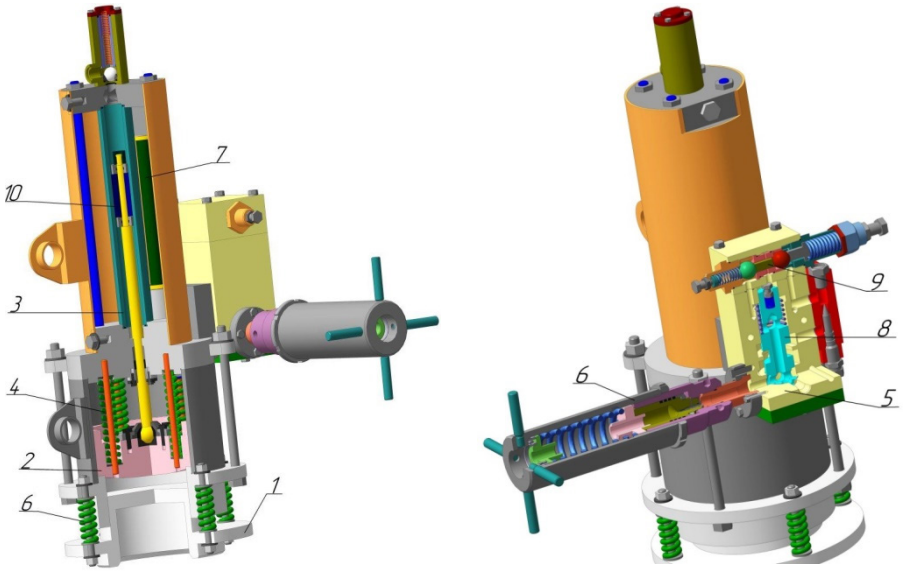

a) b)

Figure 1. *Hinged HID-based VI device: a – view of the section from the side of the executive HID body; b – sectional view from the HID side and the accumulator*

Notes: *1 – headpiece; 2 – impact mass; 3 – executive hydraulic cylinder; 4 – elastic elements; 5 – HID; 6 – accumulator; 7 – drain line; 8 – second stage; 9 – servo valves; 10 – working body*

The mounted inertial HID-based VI hammer (see Fig. 1) comprises a headpiece (1), which is connected to the pile and the impact mass (2), which is set in motion using the HID, which in turn consists of the executive hydraulic cylinder (3) and the HID (5). The HID is connected to the executive hydraulic cylinder (3) according to the "inlet" scheme (Manzhilevsky, 2019) through the hydraulic accumulator (6). This type of HID connection allows applying a power load to the working body (10) (plunger) of the executive hydraulic cylinder, which has the function of changing the impulse forces forms (Glushak *et al*., 1992). The HID working cycle begins with filling the accumulator (6), and, accordingly, accumulating pressure in it up to a certain pre-set value p_1, which is set by the control spring on the servo valves (9) of the HID (5). Having reached the specified pressure p_1, the second stage valve (8) opens in the HID (5), which connects the cavity of the accumulator (6) with the working cavity of the executive hydraulic cylinder (3). A sharp increase in pressure in the working cavity of the executive hydraulic cylinder (3) forces the working body (10) (plunger) to move upward, which forces the inertial mass (2) to rise while compressing the elastic elements (4). The movement of the inertial mass (2) upward leads to the accumulation of potential energy from the action of the forces of attraction and elastic forces. After a pressure drop p_2 in the HID system, the opening moment of which is determined according to the design parameters of the servovalves (9), the inertial mass (2) begins to move downward, which leads to shock interaction with the headgear (1), which in turn is transmitted to the count. In addition, when the pressure in the HID system drops to p_2, the working cavity of the executive hydraulic cylinder (3) is combined with the drain line (7) using the second stage valve (8). In this case, the drain line (7) is connected to the supra-plunger cavity of the actuating hydraulic cylinder (3), additionally creating loads on the plunger (10) upon the downward stroke. This design solution gives added kinetic energy to the impact mass (2), which allows increasing the energy of the shock load on the headgear (1).

To develop a mathematical model of the pile driving technology with a mounted HID-based VI device, a three-component (flat multi-mass) inertial model with contacts between masses (Fig. 2) was developed, which allows simulating elastic-plastic deformations of the soil and the stress-strain state of a pile immersed in the soil.

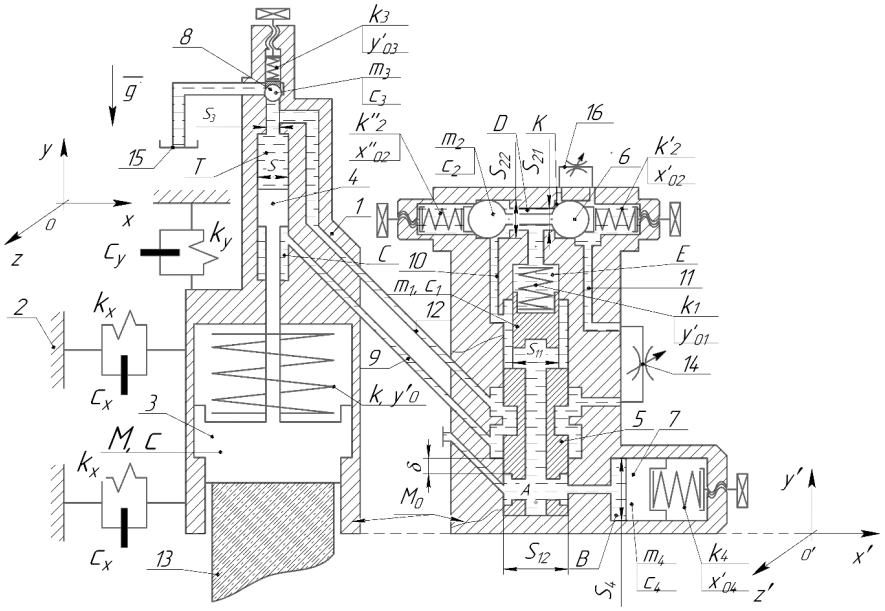

Figure 2. *Calculation model of the technological process of driving the piles of the HID-based VI device*

Notes: *1 – hull; 2 – boom vehicle; 3 – inertial mass; 4 – plunger; 5 – second stage valve; 6 – first stage valve; 7 – hydro accumulator spring; 8 – check valve spring; 9 – pressure head hydraulic lines; 10 – pressure channels; 11 – drain line; 12 – hydraulic lines; 13 – pile; 14 – throttle; 15 – hydraulic tank; 16 – first stage throttle; A – lower internal pressure chamber of the second stage valve; B – cavity of the hydro accumulator; C – pressure cavity of device 1; D – internal pressure chamber two-stage of the pulsator valve; E – upper internal pressure chamber of the second stage valve; T – drain cavity of device 1; K – internal pressure chamber of the first stage valve; c_1 – the coefficient of the forces of viscous friction between the walls of the body of the device 1 and the second stage valve 5, c_2 – the coefficient of the forces of viscous friction between the walls of the body of the VI device 1 and the first stage valve 6; c_3 – coefficient of viscous friction forces between the walls of the body of the device 1 and the check valve 8; c_4 – the coefficient of the forces of viscous friction between the walls of the body of the device 1 and the accumulator 4; c – coefficient of forces viscous friction between the walls of the body of the device 1 and the inertial mass 4; c_y, c_x – are the vertical and horizontal components of the coefficient of viscous friction forces of the damping component of the shock-absorbing unit connecting the HID device with the boom vehicle 2 (Manzhilevsky, 2019); k_1 – is the stiffness of the valve spring of the second stage 5; k'_2, k''_2 – is the stiffness of the valve spring of the first stage 6; k_3 – is the stiffness of the check valve spring 8; k_4 – is the stiffness of the accumulator spring 4; k – is the stiffness of the spring of the inertial mass 3; k_y, k_x – is the vertical and horizontal components of the stiffness of the elastic component of the shock-absorbing unit of the connecting HID device with the boom of the vehicle 2 (Thümmel, 2012); y'_{01} – is the pre-tension of the valve spring of the first stage 5; y'_0 – is the pre-tension of the inertial mass spring 3; x''_{02}, x'_{02} – is the pre-tensioning of the valve springs of the first stage 6; y'_{03} – is the pre-tension of the check valve spring 8, x'_{04} – is the pre-tension of the hydro accumulator spring 7; M_0 – mass of the device; M – mass of the inertial mass 3; m_1 – mass of the second stage valve 5; m_2 – mass of the first stage valve stage 6; m_3 – mass of the check valve 8 with; m_4 – mass of the hydro accumulator 7; S_{11} – small surface of the second stage valve 5; S_{12} – external surface of the second stage valve 5; S_{21} – small surface of the first stage valve 6; S_{22} – external surface of the first stage valve 6; S_3 – surface area of the check valve surface 8; S_4 – inner surface of the hydro accumulator plunger 7; δ – is the second stage valve overlap 5; g – acceleration of gravity*

The absolute *xOyz* and the movable coordinate system *x'O'y'z'* are introduced, which are rigidly connected to the hull (1) of the attachment with a mass M_0, and the movable coordinate system *x"O"y"z"* is rigidly connected to the submerged pile (13) (see Fig. 2). It is expedient to divide the pile driving technology with a hinged HID-based device into two periods: the period of accumulation of kinetic energy and the period of impact interaction of the inertial mass (3) by driving the pile (13) into the soil (Bingham *et al.*, 2000). The period of accumulation of the kinetic energy of the HID by the device consists of the characteristic working movements of the locking elements (5-7) and the plunger (4). In turn, the period of impact interaction is characterised by viscoplastic deformations of the soil and the stress-strain state of the pile (13). Next, this study considers the working period of the accumulation of kinetic energy in more detail. The equations of motion for body (1) of a device (see Fig. 2) with mass M_0 is written as follows:

$$\begin{cases} -M_0\ddot{y} = -M_0 g + k_1(y'_{01} + y'_1) + k_3(y'_{03} + y'_3) + k(y'_0 + y') - \\ -\iint\limits_{\tilde{S}} p_{\tilde{S}}(t)dS_y + c_y\dot{y} + c_1\dot{y}'_1 + c_3\dot{y}'_3 + c\dot{y}' - N_{05y} - N_{08y} - N_{03y}; \\ -M_0\ddot{x} = -\iint\limits_{\tilde{S}} p_{\tilde{S}}(t)dS_x + 2c_x\dot{x} + 2k_x x - k''_2\left(x''_{02} - x'_2\right) + \\ +k'_2\left(x'_{02} + x'_2\right) + k_4(x'_{04} + x'_4) + c_2\dot{x}_{02} - c_4\dot{x}'_4 - N_{06x} \end{cases} \quad (1)$$

where: $p_{\tilde{S}}(t)$ is the function of changing the pressure of the working fluid in the internal cavity hydraulic channels of the VI device; $\iint_{\tilde{S}} p_{\tilde{S}}(t)dS_y$, $\iint_{\tilde{S}} p_{\tilde{S}}(t)dS_x$ are the corresponding components of the forces, acting on the inner surface $\tilde{S}$ of the cavity of the hydraulic channels of the device; N_{05y} are the vertical components of the reaction forces of a cylindrical support of the second stage valve (5) on the body of the two-stage pulsator valve; N_{08y} are the vertical components of the reaction forces of the check valve (8) on the conical support device body (1); N_{03y} is the reaction force of the inertial mass (3) into the device body (1); N_{06x} is the horizontal component of the reaction forces of the first stage valve (6) on the body of the device (1).

The equations of motion for the inertial mass (3) weighing Mg are as follows:

$$M\ddot{y}_0 = -Mg - k(y'_0 + y'_0) + \iint\limits_S p_S(t)dS - c\dot{y}'_0 + N_{30y} \quad (2)$$

where $p_S(t)$ is the function of changing the pressure of the working fluid in the internal pressure C and drain T cavities of device (1); $\iint p_S(t)dS$ is the corresponding components of the forces, acting on the inner surfaces S of the plunger (4) of the inertial mass (3); N_{30y} is the reaction force of the device body (1) to the inertial mass (3).

Since the first stage valve (6) along the *y*-axis moves together with the body of the hinged VI device (1), the equation of motion for the first stage valve (6) with mass m_2 along the *x*-axis is as follows:

$$m_2\ddot{x}_2 = k''_2\left(x''_{02} - x'_2\right) - k'_2\left(x'_{02} + x'_2\right) - c_2\dot{x}'_2 + \iint\limits_{S_{22}-S_{21}} p_{S_{22}-S_{21}}(t)dS + N_{60x} \quad (3)$$

where $p_{S_{22}-S_{21}}(t)$ is the function of changing the pressure of the working fluid in the internal pressure chambers *D* and *K* two-stage of the pulsator valve; $\iint_{S_{22}-S_{21}} p_{S_{22}-S_{21}}(t)dS$ is the corresponding components of the forces acting on the inner surface of the S_{22}–S_{21} of the first stage valve (6); N_{60x} is the horizontal component of the reaction forces of the housing of device (1) on the first stage valve (6).

Equations of motion for the second stage valve (5) with mass m_1:

$$m_1\ddot{y}_1 = -m_1 g - k_1(y'_{01} + y'_1) - c_1\dot{y}'_1 + \iint\limits_{(S_{12}-S_{11})} p_{(S_{12}-S_{11})}(t)dS + N_{50y} \quad (4)$$

where $p_{(S_{12}-S_{11})}(t)$ is the function of changing of the pressure of the working fluid in the internal pressure chambers *A*, *E* of a two-stage pulsator valve; $\iint_{(S_{12}-S_{11})} p_{(S_{12}-S_{11})}(t)dS$ are the corresponding components of the forces acting on the area S_{12}–S_{11} of valve surface of the second stage valve (5); N_{50y} is the vertical components of the reaction forces of the device body (1) on the lower cylindrical surface of the second stage valve (5). Since the plunger valve of the accumulator (7) on the *y*-axis is moving together with the hinged device (1), the equations of motion for the plunger of the hydro accumulator (7) with mass m_4 along the *x*-axis are as follows:

$$m_4\ddot{x}_4 = -k_4\left(x'_{04} + x'_4\right) - c_4\dot{x}'_4 + \iint\limits_{S_4} p_{S_4}(t)dS \quad (5)$$

where $p_{S_{22}-S_{21}}(t)$ is the function of changing the pressure of the working fluid in the internal pressure chambers D and K of the two-stage pulsator valve; $\iint_{S_4} p_{S_4}(t)dS$ is the corresponding components of the forces acting on the inner surface S_4 of the plunger of the hydro accumulator (7).

Equations of the motion for check valve (8) with mass m_3 are as follows:

$$m_3\ddot{y}_3 = N_{80y} - k_3(y'_{03} + y'_3) - c_3\dot{y}'_3 + \iint_{S_3} p_{S_3}(t)dS - m_3 g \tag{6}$$

where $p_{S_3}(t)$ is the function of changing of the pressure of the working fluid in the internal pressure chambers *A*, *E* of the two-stage pulsator valve; $\iint_{S_3} p_{S_3}(t)dS$ are the corresponding components of the forces acting on the surface area S_3 of the surface of the check valve (8); N_{80y} are the vertical components of the reaction forces of the device body (1) on the conical surface of the check valve (8). In this case, it is a neglect of the inertial forces of the working fluid acting on the working parts of the HID as bearing an insignificant contribution to the changes of the device movement in general. To fully write down the mathematical model of the VI device operation, it is necessary that the operation of the HID for the corresponding working phases of the two-stage of the pulsator valve is considered.

Pressure build-up phase. In this phase, the first stage valve (6) and second stage valve (5), as well as the inertial mass (3) with the check valve (8) are at rest. At this phase, the second stage valve (5) overclocks the pressure chambers *A* and *C*, causing a pressure build-up in the cavity *B* of the hydro accumulator (7). In this case, the cavity A is connected to the cavities D and E through the pressure channels (10). The initial conditions for this phase $0 \le t \le t_{sp}$ are as follows:

$$\begin{cases} \iint_{S_{22}-S_{21}} p_{S_{22}-S_{21}}(t)dS \le k''_2 x''_{02} - k'_2 x'_{02}; \iint_{(S_{12}-S_{11})} p_{(S_{12}-S_{11})}(t)dS \le k_1 y'_{01}; \iint_{S_3} p_{S_3}(t)dS \le k_3 y'_{03}; \\ \dot{y}'_0(t) = \dot{y}'_1(t) = \dot{y}'_3(t) = 0; \dot{x}'_2(t) = 0; 0 \le x'_4(t) \le x'_{4\max} \end{cases} \tag{7}$$

where $x'_{4\max}$ is the maximum stroke of the plunger of the hydro accumulator (7).

Pulsator valve actuation phase. In this phase, the first stage valve (6) opens, since the pressure in the cavity D acting on the working area S_{22}–S_{21} got equated with the force adjustment of the springs $k''_2 x''_{02} - k'_2 x'_{02}$. The first stage valve (6) leads to a pressure change in cavity *E*, causing a pressure drop across the working area S_{12}–S_{11} of the second stage valve (5) and making it move upward.

For this phase $t_{sp} \le t \le t_w$, the initial conditions (Eq. 8) are written. The phase of the rise of the inertial mass (3). At this phase, there is a communication between the pressure cavities A, B, and the cavity C. At the same time, the internal cavities D, K, E are connected through the drain lines (11-12) and a throttle (14) with a drain cavity T. The combination of cavities A, B, and C through the piston (4) makes the inertial mass (3) move up:

$$\begin{cases} \iint_{S_{22}-S_{21}} p_{S_{22}-S_{21}}(t)dS \ge k''_2 x''_{02} - k'_2 x'_{02}; \iint_{(S_{12}-S_{11})} p_{(S_{12}-S_{11})}(t)dS \ge k_1 y'_{01}; \iint_{S_3} p_{S_3}(t)dS \le k_3 y'_{03}; \\ \dot{y}'_0(t) = \dot{y}'_3(t) = 0; \ 0 \le y'_1(t) \le \delta; N_{60x} = N_{06x} = 0; \\ N_{05y} = N_{50y} = 0; 0 \le x'_2(t) \le x'_{2\max}; 0 \le x'_4(t) \le x'_{4\max} \end{cases} \tag{8}$$

where $x'_{2\max}$ is the maximum stroke of the first stage valve (6), δ is the overlap of the second stage valve (5).

For this phase $t_w \le t \le t_{el}$, the following initial conditions are recorded as follows:

$$\begin{cases} \iint_{S_{22}-S_{21}} p_{S_{22}-S_{21}}(t)dS \ge k''_2 x''_{02} - k'_2 x'_{02}; \iint_{(S_{12}-S_{11})} p_{(S_{12}-S_{11})}(t)dS \ge k_1 y'_{01}; \\ \iint_{S_3} p_{S_3}(t)dS \ge k_3 y'_{03}; \delta \le y'_1(t) \le y'_{1\max}; \ 0 \le x'_2(t) \le x'_{2\max}; \\ 0 \le x'_4(t) \le x'_{4\max}; \ 0 \le y'_0(t) \le y'_{0\max}; \ 0 \le y'_3(t) \le y'_{3\max}; \\ N_{05y} = N_{50y} = 0; N_{06x} = N_{60x} = 0; N_{08y} = N_{80y} = 0; N_{30y} = N_{03y} = 0 \end{cases} \tag{9}$$

where $y'_{1\max}$ is the maximum stroke of the second stage valve (5); $y'_{0\max}$ is the maximum stroke of inertial mass (3); $y'_{3\max}$ is the maximum stroke of the check valve (8).

The phase of lowering the inertial mass (3). At this phase, there is a drop in pressure in the cavity *C* and through the hydraulic lines (9, 12) the working fluid flows into the drain cavity T and, accordingly, into the hydraulic tank (15). At the same time, the first stage valve (6) returns to the initial position and causes the overlap of the cavities K and D, while the throttle (16) allows the working fluid to drain into the drain line (11). After the overlap of the cavities K and D, the pressure in

the cavity E drops, which forces the second stage valve (5) to rotate to its original position.

For this phase $t_{el} \le t \le t_{ds}$, the initial conditions (10) are recorded as follows:

$$\begin{cases} \iint\limits_{S_{22}-S_{21}} p_{S_{22}-S_{21}}(t)dS \ge k_2'' x_{02}'' - k_2' x_{02}'; \quad \iint\limits_{(S_{12}-S_{11})} p_{(S_{12}-S_{11})}(t)dS \ge k_1 y_{01}'; \\ \iint\limits_{S_3} p_{S_3}(t)dS \ge k_3 y_{03}'; \ 0 \le y_1'(t) \le y_{1\max}'; \ 0 \le x_2'(t) \le x_{2\max}'; \\ 0 \le x_4'(t) \le x_{4\max}'; \ 0 \le y_0'(t) \le y_{0\max}'; \ 0 \le y_3'(t) \le y_{3\max}'; \\ N_{05y} = N_{50y} = 0; N_{06x} = N_{60x} = 0; N_{08y} = N_{80y} = 0; N_{30y} = N_{03y} = 0. \end{cases} \tag{10}$$

The period $t_{ds} \le t \le t_{dp}$ of the impact interaction of the inertial mass (3), the immersed pile (13) with the soil (17), is being considered (Fig. 3). Experimental studies of the immersion impact of piles (Manzhilevsky, 2019; Goncharevich, 1981) indicate that the immersion occurs as follows. During the inertial movement of the submerged pile (13), deformation of the soil occurs upon contact with the conical surface of the submerged pile with an inner cone angle α. Multiple frequency deformations of the contacting soil layer (17) contribute to the opening of internal cracks and to the accumulation of residual deformations, which, as a result, reduce the fracture stress and contribute to a relative displacement with subsequent compaction of the contacting soil layers (17) with the surface of the submerged pile (13). Considering the given regularities of the submersion process, a phenomenological model of the soil layer has been developed, which is subjected to shock strain from the conical surface of the submerged pile (13) (see Fig. 3). The soil model is a trimass-elasto-viscoplastic rheological body (Israelashvili, 2004; Magnus *et al.*, 2008). Elastic deformations of the model are reproduced by radially distributed elastic elements with vertically and horizontally constituent stiffness coefficients k_y and k_x, and dampers with vertically and horizontally constituting viscous resistance coefficients c_x and c_y, respectively.

The process of deformation (destruction) and displacement of the two-mass model of the soil layer in projections on the *x*, *y* axis at the stage $t_{ds} \le t \le t_{ed}$ spring-viscous deformation of the soil layer is described by a system of differential equations as follows:

$$\begin{cases} (1-\lambda)\xi m\ddot{x} = N_{13,17x} - c_x(\dot{x}-\dot{x}_0) - k_x(x-x_0); \\ (1-\lambda)\xi m\ddot{y} = N_{13,17y} - c_y(\dot{y}-\dot{y}_0) - k_y(y-y_0), \end{cases} \tag{11}$$

where (1-λ)ξm is the vibrational free mass of the soil layer 17; *x*, *y* are the mass movement (1-λ)ξm towards *x*, *y* axes; x_0, y_0 are the mass movement $\lambda\xi m$ towards the axes x_0, y_0; $N_{13,17y(x)}$ are the components of the reaction forces of pile 13 with soil 17 from the interaction with a conical surface *I–I*.

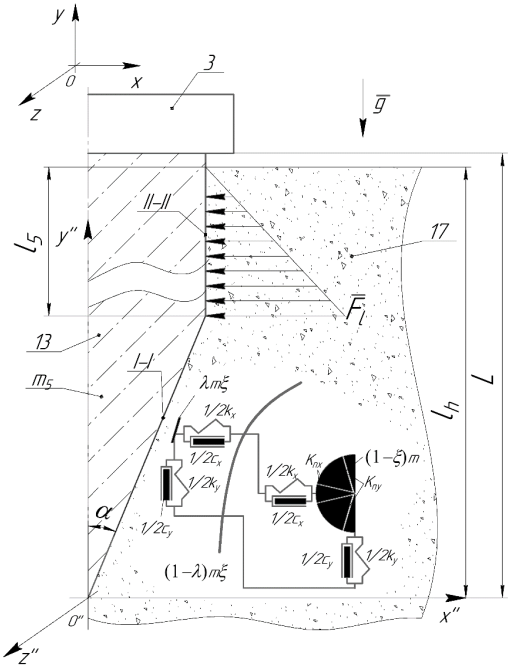

***Figure 3**. Dynamic model of the VI pile driving*

***Notes**: 3 – inertial mass; 13 – pile; 17 – soil; I-I – conical pile surface; II-II – cylindrical submerged in the ground 17 pile surface 13; k_y, k_x – vertically and horizontally constituent stiffness coefficients, respectively; c_y, c_x – vertically and horizontally constituting viscous resistance coefficients, respectively; (1-ξ) m – specific gravity of interacting soil 17; (1-λ)ξm – is the vibrational free mass of the soil layer 17; λmξ – mass of the contacting soil layer 17; $k_{\alpha y}$ i k_{nx} – are the vertical and horizontal components of the deformation coefficients; m_5 – mass of the pile 13; α – pile cone angle; l_h – submerged pile length; l – total pile length; l_5 – length of the vertical part of the pile buried in the ground; F_l – specific reaction force of the soil 17 during the interaction of piles 13 along the vertical plane II-II; g – acceleration of gravity*

Plastic deformations of the soil layer 17 at the stage $t_{ed} \le t \le t_{pd}$ are described by the following equations:

$$\begin{cases} (1-\lambda)\xi m\ddot{x} = N_{13,17x} - k_{nx}(x - x_{\kappa}^{n6}); \\ (1-\lambda)\xi m\ddot{y} = N_{13,17y} - k_{ny}(y - y_{\kappa}^{n6}) \end{cases} \quad (12)$$

where k_{ny} і k_{nx} are the vertical and horizontal components of the deformation coefficients.

Equations of motion for the *y*-axis of the pile 13 of the VI device with mass m_5 is as follows:

$$m_5\ddot{y} = m_5 g + N_{3,13} - N_{17,13}(\sin\alpha + \mu_y) - \mu_y \int_0^{l_5} F_l dy \quad (13)$$

where $\int_0^{l_5} F_l dy$ is the reaction force of the soil (17) with interaction with the pile 13 along the vertical plane *II-II*; μ_y is the vertical component of the soil (17) and pile (13) friction coefficient; $N_{17,13}$ is the component of the reaction forces of the soil (17) from the interaction with the conical surface *I-I* of the pile (13); $N_{3,13}$ is a compound of the reaction forces of the inertial mass (3) with the upper base of the pile (13).

DISCUSSION

The mathematical model of the pile driving technology involving a HID-based VI device, which is represented by the systems of equations (1-13) and additionally by the Navier-Stokes hydrodynamics equations (Iskovych-Lototsky *et al.*, 2018b; Iskovich-Lototsky *et al.*, 2019), was implemented according to numerical modelling methods based on software systems FlowVision (Iskovich-Lototsky *et al.*, 2019), Matlab Simulink (Iskovych-Lototsky *et al.*, 2018a; Shatokhin *et al.*, 2019) powered by computing clusters of the V.M. Glushkov CS Institute of Cybernetics of the NAS (National Academy of Sciences) of Ukraine (Yarovyy *et al.*, 2012). The result of the calculation in the FlowVision software package was the distribution of pressure (Fig. 4, a) and velocity (Fig. 4, b) of the working fluid in the HID cavities.

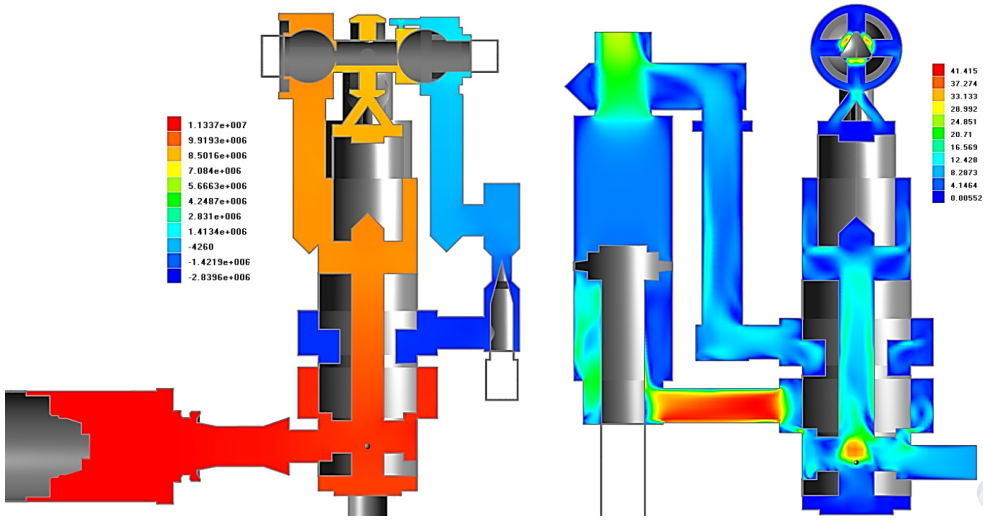

a) b)

Figure 4. *Distribution of pressure (a) and velocity (b) of the working fluid in the HID cavity of the VI device for pile driving*

The numerical result of the calculation in the FlowVision software package is the diagrams of changes in the integral value of pressure in various HID cavities of a VI device for pile driving (Fig. 5).

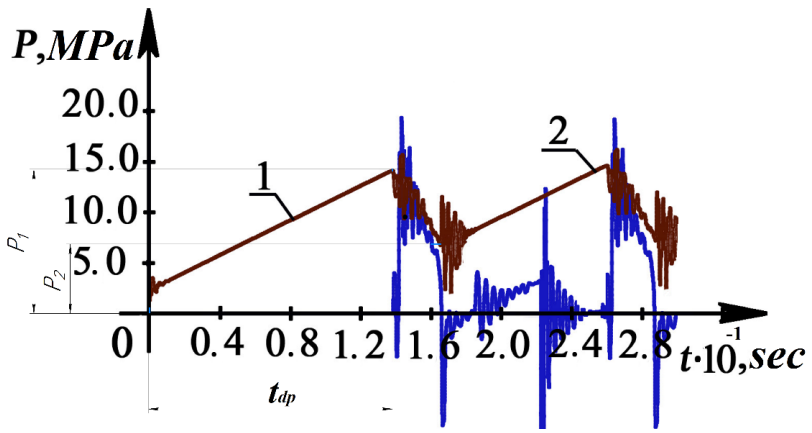

Figure 4. *Diagrams of pressure changes in the HID cavities of the VI device for pile driving*

Notes: *1 – change in pressure in the accumulator cavity; 2 – pressure change in the pressure chamber of the executive hydraulic cylinder; t_{dp} – charging time of the accumulator; p_1 – pressure pulsation amplitude in the executive hydraulic cylinder; p_2 – pressure pulsation amplitude in the accumulator*

The next result of the calculation in the FlowVision software package is the diagrams of changes in the movement of the moving elements of the HID of the VI device for pile driving (Fig. 6).

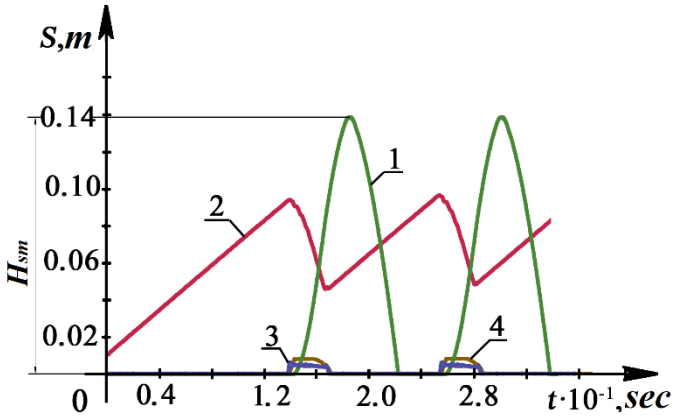

Figure 6. *Diagrams of changes in the movement of movable elements of the HID of a VI device for pile driving*

Notes: *1 – change in the displacement of the impact mass; 2 – change in the movement of the accumulator; 3 – change in the movement of the first stage valve; 4 – change in the movement of the second stage valve; H_{sm} – oscillation amplitude of the impact mass*

Additionally, using the Matlab Simulink software package, motion diagrams (Fig. 7) of a pile submerged into a soil layer of the "quartz sand" type were obtained during a two-time impact interaction.

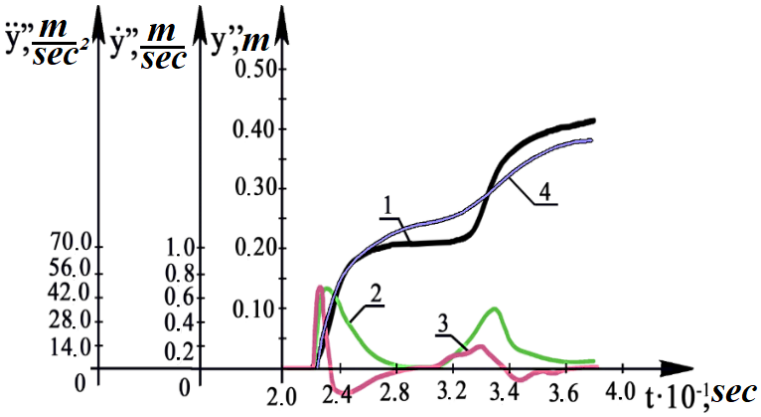

Figure 7. *Diagrams of the change in the kinematic parameters of the pile submerged during operation of the HID-based VI device*

Notes: *1 – change in the movement of the submerged pile; 2 – change in the speed of the pile submerged driven; 3 – change in the acceleration of the submerged pile; 4 – experimental data on changes in the displacement of a submerged pile (Manzhilevsky, 2019; Guo et al., 2014)*

In the middle of the second stage valve cavity (8) (see Fig. 1), the pressure is considerably higher than in the lower cavity of the first stage valve (9), and this difference is approximately 1.5 MPa (see Fig. 4, a). This pressure difference creates an added force that allows the second stage valve (9) to move while connecting the pressure cavities of the accumulator 6 and the hydraulic cylinder (3). It is also noted that the pressure in the drain channel after the first stage valve (9) is 1.5 MPa is bigger than in the main drain channel (7) of the HID (see Fig. 4, a). This fact indicates the high efficiency of the throttle assembly (14) (see Fig. 1). The use of an added control stage in the form of the first stage valve allows considerably reducing the dimensions and, accordingly, the total weight of the control hydraulic equipment. Figure 4, b, demonstrates the extreme velocity values in the pressure channel (9) of the executive hydraulic cylinder (3) (see. Fig. 1), which is a consequence of the movement of the total flows of the working fluid from the hydraulic pump and accumulator. The second stage valve (8) is under an additional action of a dynamic force occurring from the velocity head in the middle of the valve itself at the conical chamfer. This added component of the hydrodynamic force requires an additional increase in the rigidity of the elastic element of the second stage valve (8) (see Fig. 1).

The analysis of the pressure diagrams (see Fig. 5) demonstrates that at the opening phase of the second stage valve (8) (see Fig. 1), the pressure in the pressure cavity of the actuating hydraulic cylinder (3) is 3 MPa more than the maximum pressure in the cavity of the accumulator (6), which is a consequence of hydraulic shock (Wilcox, 1994; Teng *et al.*, 2010). In addition, during the second period of the pressure drop phase in the

pressure cavity of the actuating hydraulic cylinder (3), there is a certain pressure drop by 2 MPa compared to the nominal initial pressure in the hydraulic system. This phenomenon indicates the presence of weakness in the working fluid (Wilcox, 1994; Sevostianov *et al*., 2021). The presence of pressure pulsations in the second phase of the pressure drop (see Fig. 5), both in the cavity of the accumulator (6) and in the pressure cavity of the actuating hydraulic cylinder (3) (see Fig. 1) indicates the presence of accumulated resonance phenomena in the working fluid and is the result of the presence of wave processes in a moving working fluid (Iskovych-Lototsky *et al*., 2018a; Iskovych-Lototsky *et al*., 2018b; Wilcox, 1994). The diagram in Figure 5 suggests that the amplitude of the pressure pulsations for the pressure cavity the accumulator p_2=8 MPa, and for the pressure chamber of the executive hydraulic cylinder p_1=12 MPa. The accumulator build-up time (energy storage time) is t_{dp}=0.14 s.

Analysis of the diagrams of changes in the displacement of the movable elements of the HID of the VI device for pile driving (see Fig. 6) allows determining the following operating parameters of the technological process:

– the oscillation amplitude of the impact mass of the HID H_{sm}=140.6 mm, the first stage valve – 6.0 mm; the second stage valve – 8.0 mm; hydroaccumulator – 48.2 mm;

– the frequency of operation (vibration) of the shock mass and, accordingly, the device itself is 5.8 Hz.

The diagram of the change in the kinematic parameters of the pile being driven during the operation of the HID-based VI device (see Fig. 7) suggests that the depth of immersion during the first shock interaction, on average, is 0.23 m, and during the second – 0.18 m. Average pile sinking speed at the first impact interaction is 0.4 m/s, and at the second – 0.27 m/s. The average acceleration of pile sinking during the first impact interaction is 35.0 m/s^2, and at the second – 28.0 m/s^2. Average error in approximating the change in the displacement of a submerged pile in a soil medium of the "quartz sand" type in comparison with experimental data amounted to 10.40% (Manzhilevsky, 2019; Guo *et al*., 2014), which allows considering the developed mathematical models highly adequate to real systems (Mori, 2017; Palm, 2007; Shabana, 2019; Spreemann & Manoli, 2012).

CONCLUSIONS

As a result of the performed research, the authors of this paper offer a design of a VI device for pile driving with a highly efficient and compact HID based on two-stage pulsator valve. A mathematical model has been improved for studying the pile driving technology for a HID device based on the laws of hydrodynamics using mechanoreological phenomenology and generalised laws of mechanics.

Based on the developed mathematical model by finite volume methods using numerical modelling, working dependences were obtained to determine the main performance characteristics of the pile driving technology using the HID-based VI device. Comparative results of numerical modelling of the pile driving technology demonstrated the advantages of the chosen design approach and proved the efficiency of the developed HID design based on a two-stage pulsator valve.

REFERENCES

[1] Alessandro, D. (2016). Modelling and experimental validation of a nonlinear proportional solenoid pressure control valve. *International Journal of Fluid Power*, 17, 90-101. doi: 10.1080/14399776.2016.1141636.
[2] Barkan, D.D. (1952). Experimental studies of immersion in soil of piles, sheet piles and pipes. *Mechanisation of Construction*, 5, 31-36.
[3] Bingham, C., Stone, D., Schofield, N., Howe, D., & Peel, D. (2000). Amplitude and frequency control of a vibratory pile driver. *IEEE Transactions on Industrial Electronics*, 47(3), 623-631 doi: 10.1109/41.847903.
[4] Bullock, R.L., & William, A.H. (2001). *Underground mining methods: Engineering fundamentals and international case studies*. Littleton: SME.
[5] Fossen, T.I., & Nijmeijer, H. (2012). *Parametric resonance in dynamical systems*. New York: Springer. doi: 10.1007/978-1-4614-1043-0.
[6] Glushak, B.L., Novikov, S.A., Riazanov, A.I., & Sadurin, A.I. (1992). *Destruction of deformable media under impulse loads*. Nizhny Novgorod: Nizhny Novgorod University.
[7] Goncharevich, I.F. (1981). *Theory of vibration engineering and technology*. Moscow: Nauka.
[8] Guang, L., & Min, W. (2005). Modelling and controlling of a flexible hydraulic manipulator. *Journal of Central South University of Technology: Science & Technology of Mining and Metallurgy*, 12(5), 578-583.
[9] Guo, Y.S., Zhang, Y., & Cheng, M.K. (2014). Hammer rod optimisation of large tonnage air hammer. *Applied Mechanics and Materials*, 644-650, 81-84. doi: 10.4028/www.scientific.net/amm.644-650.81.
[10] Iskovich-Lototsky, R., Kots, I., Ivanchuk, Y., Ivashko, Y., Gromaszek, K., Mussabekova, A., & Kalimoldayev, M. (2019). Terms of the stability for the control valve of the hydraulic impulse drive of vibrating and vibro-impact machines. *Przeglad Elektrotechniczny*, 4(19), 19-23. doi: 10.15199/48.2019.04.04.

[11] Iskovych-Lototsky, R.D., Ivanchuk, Y.V., Veselovska, N.R., Surtel, W., & Sundetov, S. (2018a). Automatic system for modelling vibro-impact unloading bulk cargo on vehicles. *Proceedings of SPIE – The International Society for Optical Engineering,* 10808, article number 1080860. doi: 10.1117/12.2501526.
[12] Iskovych-Lototsky, R.D., Ivanchuk, Y.V., Veselovsky, Y.P., Gromaszek, K., & Oralbekova, A. (2018b). Automatic system for modelling of working processes in pressure generators of hydraulic vibrating and vibro-impact machines. *Proceedings of SPIE – The International Society for Optical Engineering,* 10808, article number 1080850. doi: 10.1117/12.2501532.
[13] Israelashvili, J. (2004). *Intermolecular and surface forces*. London: Academic Press.
[14] Ivanchuk, Ya.V. (2020). *Biomass as raw material for production of biofuels and chemicals*. London: Balkema book. doi: 10.1201/9781003177593.
[15] Jörg, C., Mont, K., & Pornsak, S. (2010). Response analysis of nonlinear vibro-impact system coupled with viscoelastic force under colored noise excitations. *Chemical Engineering Research and Design*, 88(1), 100-108. doi: 10.1016/j.cherd. 2009.07.001.
[16] Kang, S.H., Park, S.J., & Jung, S.G. (2008). Experimental Study on vibration reduction estimation of PRD Pile driving method PRD pile driving. *Transactions of the Korean Society for Noise and Vibration Engineering*, 18(7), 775-782.
[17] Li, A., Dai, F., Xu, N., Gu, G., & Hu, Z. (2019). Analysis of a complex flexural toppling failure of large underground caverns in layered rock masses. *Rock Mechanics and Rock Engineering*, 52(9), 3157-3181. doi: 10.1007/s00603-019-01760-5.
[18] Magnus, K., Popp, K., & Sextro, W. (2008). *Schwingungen: Eine Einführung in die physikalischen Grundlagen und die theoretische Behandlung von Schwingungsproblemen*. Wiesbaden: Vieweg+Teubner Verlag.
[19] Manzhilevsky, O.D. (2019). Analysis of hydraulic vibration drive machine for vibration abrasive processing. *Przeglad Elektrotechniczny*, 1(4), 95-99. doi: 10.15199/48.2019.04.16.
[20] Mori, Y. (2017). *Mechanical vibrations: Applications to equipment*. London: ISTE.
[21] Palm, W.J. (2007). *Mechanical vibration*. Hoboken: John Wiley.
[22] Sevostianov, I.V., Ivanchuk, Y.V., Polishchuk, O.V., Lutsyk, V.L., Dobrovolska, K.V., Smailova, S., Wójcik, W., & Kalizhanova, A. (2021). Development of the Scheme of the Installation for Mechanical Wastewater Treatment. *Journal of Ecological Engineering*, 22(1), 20-28. doi: 10.12911/22998993/128693.
[23] Shabana, A.A. (2019). *Theory of vibration: An introduction*. Dordrecht: Springer.
[24] Shatokhin, V.M., Sobol, V.N., Wujcik, W., Mussabekova, A., & Baitussupov, D. (2019). Dynamical processes simulation of vibrational mounting devices and synthesis of their parameters. *Przeglad Elektrotechniczny*, 4(19), 86-92. doi: 10.15199/48.2019.04.15.
[25] Spreemann, D., & Manoli, Y. (2012). *Electromagnetic vibration energy harvesting devices: Architectures, Design, Modelling and Optimisation*. Dordrecht: Springer.
[26] Teng, Y.N., Li, X.P., Zeng, Q.H., & Wen, B.C. (2010). Investigation on nonlinear dynamics characteristics of vibration friction system based on vibration pile driver. *Applied Mechanics and Materials*, 29-32, 2189-2193. doi: 10.4028/www.scientific.net/AMM.29-32.
[27] Thümmel, T. (2012). Experimentelle mechanismendynamik: Messung, modellierung, simulation. *Verifikation, Interpretation und Beeinflussung Typischer Schwingungsphänomene an Einem Mechanismenprüfstand*. Düsseldorf: VDI-Verl.
[28] Voskresenskiy, E.V. (2001). *Asymptotic methods: Theory and applications*. Saransk: SVMO.
[29] Wilcox, D.C. (1994). *Turbulence modelling for CFD*. Mumbai: DCW Industries.
[30] Yarovyy, A.A., Timchenko, L.I., & Kokriatskaia, N.I. (2012). Parallel-hierarchical computing system for multi-level transformation of masked digital signals. *Advances in Electrical and Computer Engineering*, 12(3), 13-20. doi: 10.4316/AECE.2012.03002.

Моделювання технологічного процесу занурення паль віброударним пристроєм з гідроімпульсним приводом

Ярослав Володимирович Іванчук, Олександр Дмитрович Манжілевський, Руслан Станіславович Белзецький, Олександр Дмитрович Замковий, Роман Ігорович Павлович

Вінницький національний технічний університет
21021, вул. Хмельницьке шосе, 95, м. Вінниця, Україна

Анотація. Розроблена математична модель технологічного процесу роботи віброударного пристрою для занурення будівельних паль на базі гідроімпульсного приводу. На основі аналізу розробленої математичної моделі запропоновано оптимальні режими роботи вібраційного пристрою для забезпечення інтенсифікації процесу занурення паль. Запропоновано оригінальну конструкцію сучасного високоефективного пристрою для занурення будівельних паль, який оснащено компактним потужним гідроімпульсним приводом. Для розробки математичної моделі технологічного процесу занурення паль використовувались методи механореологічної феноменології, гідродинаміки і узагальнені закони механіки. Удосконалено математичні моделі динаміки технологічних процесів занурення паль віброударним пристроєм на базі гідроімпульсного привода, у формі просторово-нестаціонарної постановки задачі та інтегральних рівнянь динамічних характеристик рухомих елементів привода. На основі розробленої математичної моделі методом кінцевих об'ємів, за допомогою чисельного моделювання і високопродуктивних обчислювальних комп'ютерних систем, отримано розподіл тиску і швидкості робочої рідини в гідроімпульсному приводі віброударного пристрою, а також зміни кінематичних параметрів елементів технологічного обладнання. Запропоновано оптимальні режими роботи гідроімпульсного приводу віброударного пристрою для забезпечення інтенсифікації технологічного процесу занурення паль. Встановлено, що при застосуванні низькочастотної вібрації відбувається інтенсифікація процесу занурення будівельних паль. Застосування гідроімпульсного приводу на основі двокаскадного віброзбудження дозволило реалізувати віброударний режим роботи пристрою. Середня швидкість занурення палі за ударно-вібраційної взаємодії у середньому в п'ять разів вища порівняно з традиційними методами занурення

Ключові слова: імпульс, удар, вібрації, математична модель, гідропривод, клапан, будівельна паля